⌘ *Author's Choice*

THE JOURNAL OF BIOLOGICAL CHEMISTRY VOL. 291, NO. 29, pp. 14986–14995, July 15, 2016

Autocrine Signaling Underlies Fast Repetitive Plasma Membrane Translocation of Conventional and Novel Protein Kinase C Isoforms in β Cells*

Received for publication, October 14, 2015, and in revised form, May 14, 2016 Published, JBC Papers in Press, May 20, 2016, DOI 10.1074/jbc.M115.698456

Anne Wuttke, Qian Yu, and Anders Tengholm[1]

From the Department of Medical Cell Biology, Uppsala University, Biomedical Centre, Box 571, 75123 Uppsala, Sweden

PKC signaling has been implicated in the regulation of many cell functions, including metabolism, cell death, proliferation, and secretion. Activation of conventional and novel PKC isoforms is associated with their Ca^{2+}- and/or diacylglycerol (DAG)-dependent translocation to the plasma membrane. In β cells, exocytosis of insulin granules evokes brief (<10 s) local DAG elevations ("spiking") at the plasma membrane because of autocrine activation of $P2Y_1$ purinoceptors by ATP co-released with insulin. Using total internal reflection microscopy, fluorescent protein-tagged PKCs, and signaling biosensors, we investigated whether DAG spiking causes membrane recruitment of PKCs and whether different classes of PKCs show characteristic responses. Glucose stimulation of MIN6 cells triggered DAG spiking with concomitant repetitive translocation of the novel isoforms PKCδ, PKCε, and PKCη. The conventional PKCα, PKCβI, and PKCβII isoforms showed a more complex pattern with both rapid and slow translocation. K^+ depolarization-induced PKCε translocation entirely mirrored DAG spiking, whereas PKCβI translocation showed a sustained component, reflecting the subplasma membrane Ca^{2+} concentration ($[Ca^{2+}]_{pm}$), with additional effect during DAG spikes. Interference with DAG spiking by purinoceptor inhibition prevented intermittent translocation of PKCs and reduced insulin secretion but did not affect $[Ca^{2+}]_{pm}$ elevation or sustained PKCβI translocation. The muscarinic agonist carbachol induced pronounced transient PKCβI translocation and sustained recruitment of PKCε. When rise of $[Ca^{2+}]_{pm}$ was prevented, the carbachol-induced DAG and PKCε responses were somewhat reduced, but PKCβI translocation was completely abolished. We conclude that exocytosis-induced DAG spikes efficiently recruit both conventional and novel PKCs to the β cell plasma membrane. PKC signaling is thus implicated in autocrine regulation of β cell function.

PKC is a serine/threonine kinase important for a broad range of cellular processes (1, 2). The PKC family contains 10 isoforms that are divided into three groups depending on their mechanism of activation. Conventional PKCs (cPKCs)[2] (PKCα, βI, βII, and γ) are activated by diacylglycerol (DAG) and Ca^{2+}. Novel PKCs (nPKCs) (PKCδ, ε, η, and θ) respond to DAG but not to Ca^{2+}. The atypical isoforms (aPKCs) (PKCζ and ι/λ) are independent of both DAG and Ca^{2+} (1, 2). Pancreatic β cells, which play a pivotal role in glucose homeostasis by releasing insulin, express members of all three PKC families. There is evidence that PKCα, βII, δ, ε, ζ, and ι/λ are expressed whereas the γ isoform is not (3–10). Conflicting results have been reported regarding expression of the βI, η, and θ isoforms (3–6, 8–10), perhaps reflecting differences in species, cell lines, and methodology to examine expression.

PKCs are involved in various aspects of β cell function, like proliferation, differentiation, and death, as well as insulin secretion (11), but the precise role of various isoforms is difficult to define because of a lack of selective pharmacological tools and potential problems with compensatory mechanisms and functional redundancy in genetic ablation studies. PKC-activating phorbol esters were found early to stimulate insulin secretion (12, 13), an effect mediated by sensitization of the secretory machinery to Ca^{2+} (14, 15). Although the involvement of PKC in the regulation of insulin release by G protein-coupled receptor stimuli is well established (11), its role in glucose-stimulated secretion is controversial. Down-regulation of PKC activity has little effect on the secretory response to glucose (16, 17), and experiments with PKC inhibitors have yielded conflicting results (18–23). Studies with genetic ablation of different PKC isozymes indicate that PKCδ and ι/λ are important for insulin secretion either by direct effects on the exocytosis machinery (24) or by controlling the expression of genes important for β cell differentiation (4). However, adenoviral overexpression of wild-type and kinase-dead forms of PKCα and δ failed to affect glucose-stimulated insulin secretion in another study (18). Also, the functional importance of PKCε is unclear. Expression of a dominant negative mutant suppressed exocytosis in isolated β cells (25), and a specific PKC translocation inhibitor reduced insulin secretion from rat islets (21). However, functional ablation of the protein did not affect glucose-induced insulin secretion and even amplified that from islets treated with fatty acids (26).

* This work was supported by grants from the Swedish Research Council, the Novo Nordisk Foundation, the Swedish Diabetes Foundation, the European Foundation for the Study of Diabetes (EFSD)-MSD, the Diabetes Research & Wellness Foundation, and the Family Ernfors Foundation. The authors declare that they have no conflicts of interest with the contents of this article.

[1] To whom correspondence should be addressed: Dept. of Medical Cell Biology, Uppsala University, Biomedical Ctr., Box 571, 75123 Uppsala, Sweden. Tel.: 46-18-4714481; Fax: 46-18-4714059; E-mail: anders.tengholm@mcb.uu.se.

[2] The abbreviations used are: cPKC, conventional PKC; DAG, diacylglycerol; nPKC, novel PKC; aPKC, atypical PKC; MARCKS, myristoylated alanine-rich kinase C substrate; $[Ca^{2+}]_{pm}$, cytoplasmic Ca^{2+} concentration beneath the plasma membrane; TIRF, total internal reflection fluorescence.

Activation of conventional and nPKCs typically involves their translocation to the plasma membrane. For nPKCs, this process is mostly DAG-driven, and for cPKCs, it depends on a combination of Ca^{2+} and DAG dynamics (27, 28). We recently discovered that glucose induces rapid DAG elevations in restricted regions of the β cell plasma membrane with durations of <10 s. They reflect the exocytotic release of adenine nucleotides with autocrine feedback activation of $P2Y_1$ purinoceptors (29). Moreover, these DAG microdomains induced PKC activation, measured as translocation of fluorescence-labeled myristoylated alanine-rich C-kinase substrate (MARCKS). However, it remains unclear whether the DAG microdomains trigger PKC translocation or whether DAG spiking merely activates PKCs already present at the plasma membrane. It also remains to be establish which subclasses of PKCs are activated and whether the different isoforms respond differentially to the glucose-induced DAG signaling pattern. Therefore, we analyzed the translocation dynamics of various fluorescence-tagged PKC isoforms and DAG dynamics as well as the subplasma membrane Ca^{2+} concentration ($[Ca^{2+}]_{pm}$) in insulin-secreting β cells using total internal reflection fluorescence (TIRF) microscopy.

Results

Depolarization-induced DAG Spiking Triggers nPKC-dependent MARCKS Phosphorylation—TIRF imaging of MIN6 insulinoma cells co-expressing an mCherry-tagged DAG sensor and the PKC activity detector MARCKS-GFP showed that K^+-mediated membrane depolarization induced repetitive, brief (<10 s) and pronounced DAG elevations. Each DAG spike was associated with less rapid dissociation of MARCKS-GFP from the plasma membrane (Fig. 1, *A* and *B*). Gö 6976, an inhibitor of cPKCs, had little effect on these responses, whereas Gö 6983, targeting both conventional and nPKCs, immediately suppressed MARCKS-GFP translocation without affecting DAG spiking (Fig. 1, *A* and *B*). These data indicate that DAG spiking primarily activates nPKCs in β cells.

Glucose-induced Plasma Membrane Translocation of nPKCs Reflects DAG Spiking—MIN6-cells were next co-transfected with the DAG biosensor and different GFP-tagged PKC isoforms. All nPKCs tested (δ, ε, and η) showed rapid, transient, and repetitive glucose-induced translocation between the cytoplasm and the plasma membrane in response to glucose, whereas the muscarinic agonist carbachol induced sustained membrane association, almost perfectly mirroring simultaneously measured DAG patterns (Fig. 2, *A*–*C*). The glucose-induced DAG spikes were often spatially confined, and the nPKCs translocated specifically to the membrane regions with elevated DAG, as illustrated for PKCε in Fig. 2*D*. PKCε was further investigated to evaluate the DAG dependence of the PKC translocation. Like glucose stimulation, membrane depolarization with a high K^+ concentration resulted in parallel DAG spiking and PKCε-GFP translocation (Fig. 3*A*). Secretagogue-induced DAG spiking in β cells is due to exocytotic release of ATP with autocrine feedback activation of $P2Y_1$ purinoceptors, which in turn activates phospholipase C (29). Consistent with DAG spiking underlying the brief plasma membrane binding of PKCε, both events were prevented by the $P2Y_1$ receptor inhibitor MRS 2179 (Fig. 3*A*). Similarly, introduction of MRS 2179 before K^+ depolarization prevented the appearance of DAG spikes as well as the concomitant transient PKCε translocation (Fig. 3*B*) without affecting the sustained depolarization-induced increase of $[Ca^{2+}]_{pm}$ (Fig. 3*C*). Conversely, brief DAG increases caused by repeated 5-s applications of 0.1 μM $P2Y_1$ receptor agonist MRS 2365 caused transient translocations of PKCε to and from the plasma membrane, whereas continuous application of the drug induced sustained responses (Fig. 3*D*).

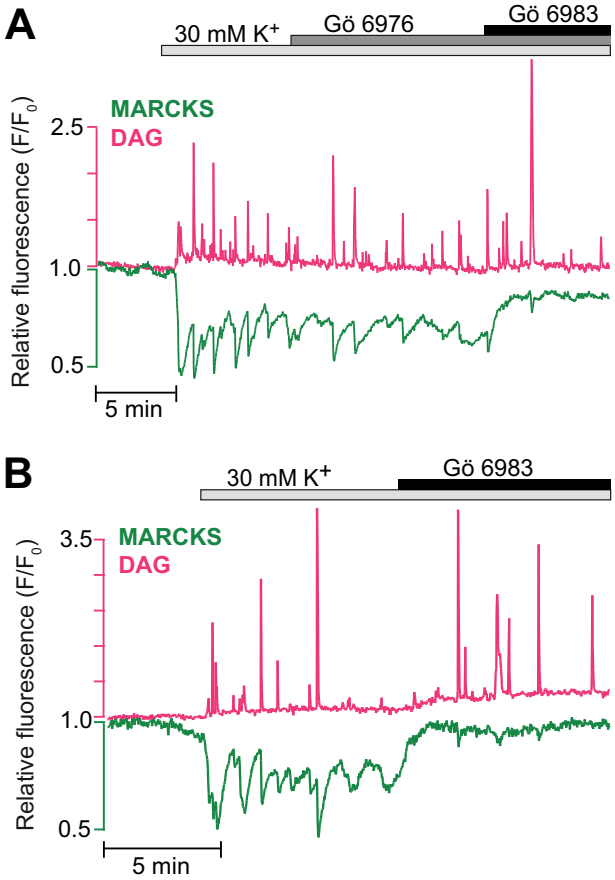

FIGURE 1. **Fast, repetitive MARCKS phosphorylation is mediated by novel PKCs.** *A* and *B*, simultaneous TIRF microscopy recordings of plasma membrane DAG concentration (*magenta*) and membrane localization of MARCKS-GFP (*green*) in single MIN6 cells. Membrane depolarization with 30 mM K^+ induced DAG spiking, which was paralleled by transient drops of MARCKS fluorescence, representing short-lived PKC activity that resulted in MARCKS phosphorylation and dissociation from the membrane. MARCKS transients were not affected by 1 μM cPKC inhibitor Gö 6976 (*A*) but vanished in response to 1 μM Gö 6983, an inhibitor of both conventional and nPKCs, when added in the presence (*A*) or absence (*B*) of Gö 6976. $n = 14$ cells in three experiments for Gö 6976 and 15 cells in five experiments for Gö 6983.

The stable acetylcholine analogue carbachol activates phospholipase C, and the resulting increases in DAG and cytoplasmic Ca^{2+} concentrations induce PKC activation. Two 5-min periods of carbachol stimulation 15 min apart resulted in comparable plasma membrane DAG increases and PKC translocation dynamics (Fig. 4*A*). PKCε-GFP translocation to the plasma membrane was sustained and typically very similar to the DAG dynamics (Fig. 4*A*). Omission of Ca^{2+} from the extracellular medium together with addition of EGTA and the Ca^{2+}-ATPase inhibitor cyclopiazonic acid to prevent elevations of the cyto-

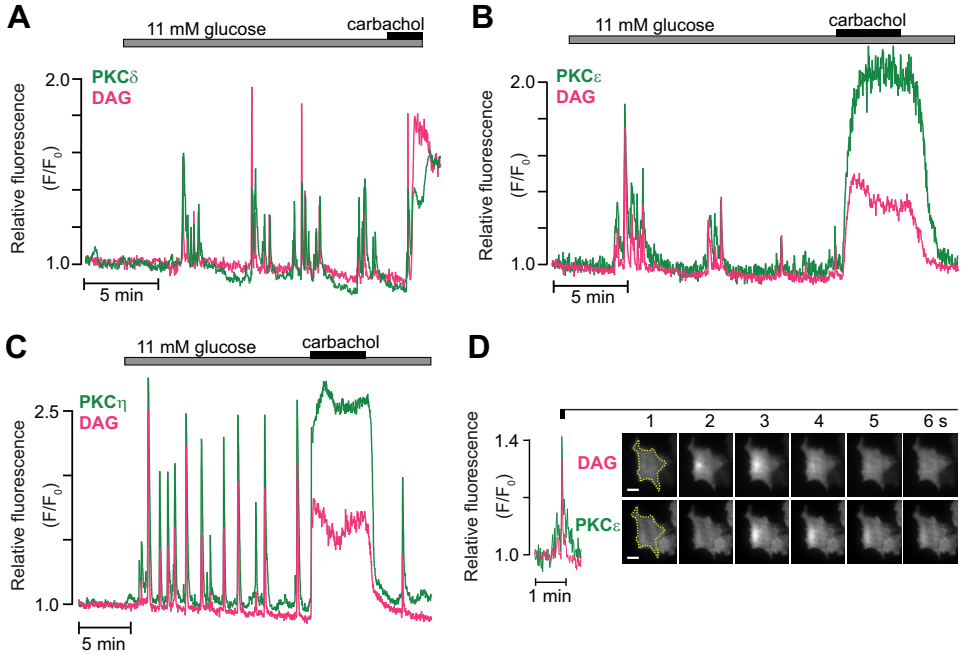

FIGURE 2. **Glucose- and carbachol-induced translocation of nPKCs.** Representative TIRF microscopy recordings from single MIN6-cells co-expressing the DAG biosensor (*magenta*) and GFP-labeled PKC (*green*) during stimulation with an increase in glucose concentration from 3 to 11 mM, followed by addition of 100 μM carbachol. *A–C*, DAG dynamics and translocation of PKCδ (*A*, $n = 7$ cells in three experiments), PKCε (*B*, $n = 8$ cells in four experiments), and PKCη (*C*, $n = 9$ cells in three experiments). *D*, TIRF image pairs acquired every second showing the spatial distribution of a DAG spike and corresponding PKCε translocation. The cell border is outlined in *yellow*. The DAG spike occurs in a restricted part of the plasma membrane, and PKCε translocates to the same region. *Scale bars* = 5 μm.

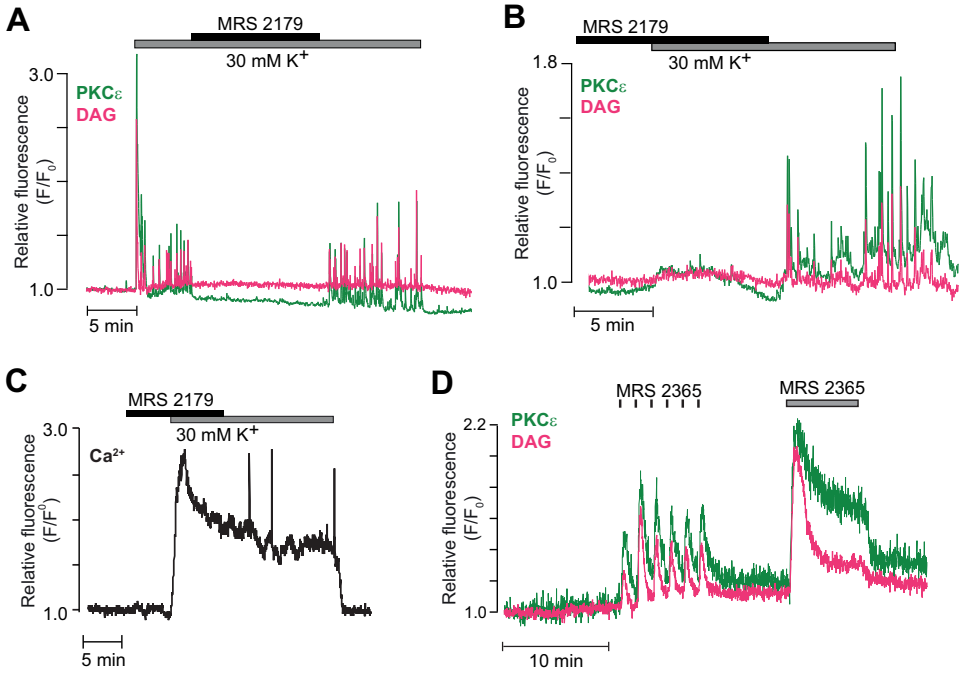

FIGURE 3. **The depolarization-induced PKCε translocation pattern reflects DAG dynamics.** Representative TIRF microscopy recordings from single MIN6 cells co-expressing the DAG biosensor (*magenta*) and GFP-labeled PKCε (*green*) or expressing the Ca^{2+} sensor R-GECO (*black*). *A* and *B*, DAG dynamics and PKCε translocation in cells exposed to 3 mM glucose, 30 mM K^+, and 10 μM of the $P2Y_1$ receptor antagonist MRS 2179. $n = 6$ cells in two experiments (*A*) and 7 cells in three experiments (*B*). *C*, single-cell recording of the $[Ca^{2+}]_{pm}$ response to depolarization with high K^+ in the presence of MRS 2179 ($n = 15$ cells from three experiments). *D*, simultaneous recording of DAG dynamics and PKCε translocation in response to repetitive applications of the $P2Y_1$ receptor agonist MRS 2365 ($n = 14$ cells from five experiments).

plasmic Ca^{2+} concentration reduced carbachol-induced DAG production, probably as a result of elimination of positive feedback from Ca^{2+} on phospholipase C (31), and PKCε-GFP translocation was consequently also slightly reduced (Fig. 4, *B* and *C*). These findings show that the glucose-induced DAG microdomains are associated with translocation of nPKCs to the plasma membrane and reinforce the notion that DAG is sufficient for driving translocation of nPKCs.

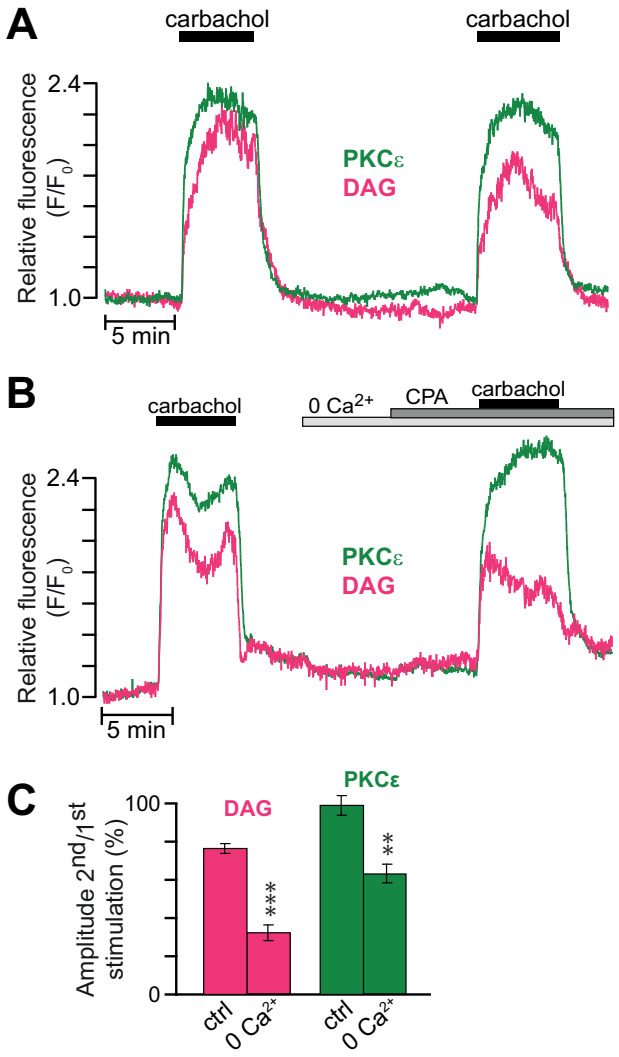

FIGURE 4. **The carbachol-induced translocation of PKCε reflects DAG dynamics.** *A*, DAG dynamics and PKCε translocation in response to repeated stimulations with 100 μM carbachol in the presence of 3 mM glucose. *B*, a similar recording but with the second stimulation made after omission of extracellular Ca^{2+} and addition of 2 mM EGTA and 50 μM cyclopiazonic acid (*CPA*). *C*, means ± S.E. for the relative amplitudes of DAG and PKCε translocation during two consecutive stimulations with carbachol in the presence or absence of Ca^{2+} as in *A* and *B* ($n = 25$ cells from three experiments and 14 cells from two experiments, respectively). **, $p < 0.0007$; ***, $p < 3 \times 10^{-5}$ for the difference from the control (*ctrl*).

Glucose Induces Complex Oscillatory cPKC Translocation Reflecting both Ca^{2+} and DAG Dynamics—Experiments were also performed with MIN6 cells co-expressing the DAG biosensor and either of the GFP-tagged cPKC isoforms PKCα, βI, or βII. Elevation of the glucose concentration to 11 mM induced prominent, repetitive translocation of all three cPKC isoforms (Fig. 5, *A–C*). The translocation pattern of PKCβII differed slightly from that of PKCα and PKCβI. Of 10 cells expressing PKCβII-GFP, four showed DAG increases and PKC translocation even at a substimulatory glucose concentration (data not shown). In the remaining cells, 11 mM glucose induced prominent, repetitive translocation of PKCβII to the plasma membrane with kinetics strikingly similar to that of DAG, and few glucose-induced PKCβII recruitments to the membrane occurred without a concomitant DAG spike (Fig. 5*B*). Carbachol triggered pronounced and sustained recruitment of PKCβII to the plasma membrane, mirroring the DAG dynamics (Fig. 5*B*).

The translocation pattern of PKCβI consisted of a small, sustained increase of fluorescence with superimposed, very pronounced (>3-fold increases in fluorescence) repetitive translocation peaks that only partially reflected parallel DAG spiking (Fig. 5, *C* and *D*). Although carbachol transformed the DAG pattern to a sustained increase, PKCβI continued to show fast, repetitive translocation from an elevated level that sometimes fluctuated slowly (Fig. 5, *C* and *D*). The fast PKCβI translocations that did not coincide with DAG spikes are most likely driven by rapid glucose-induced changes in the cytoplasmic Ca^{2+} concentration. Fig. 5, *E* and *F*, shows an example of a glucose-stimulated cell with slow oscillations of PKCβI translocation (duration >1 min) and superimposed spiking almost perfectly mirroring slow and fast oscillations of $[Ca^{2+}]_{pm}$. With PKCβI, it was more difficult to observe spatially restricted translocation coinciding with DAG microdomains than it was with the nPKCs. This was because PKCβI translocation spikes were so frequent and clearly dependent on factors in addition to DAG. Fig. 5*G* shows one of the rather infrequent examples of an isolated PKCβI translocation event paralleled by local DAG generation.

Membrane depolarization with a high K^+ concentration resulted in sustained plasma membrane translocation of PKCβI-GFP with superimposed spiking (Fig. 6*A*). This PKCβI-GFP spiking was inhibited when DAG spiking was prevented by $P2Y_1$ receptor inhibition with MRS 2179 (Fig. 6, *A* and *B*). However, the sustained translocation of PKCβI-GFP was unaffected by the drug (Fig. 6*A*), showing dynamics strikingly similar to those of $[Ca^{2+}]_{pm}$, with a slight time-dependent decline (Fig. 6, *C* and *D*). Likewise, introduction of MRS 2179 before K^+ depolarization did not affect the subsequent $[Ca^{2+}]_{pm}$ elevation and stable PKCβI translocation but prevented the appearance of rapid DAG and $[Ca^{2+}]_{pm}$ spikes as well as the concomitant transient PKCβI translocations (Fig. 6, *E* and *F*).

In the presence of 3 mM glucose, carbachol triggered an initial distinct peak of PKCβI-GFP translocation to the plasma membrane, followed within a few seconds by dissociation and stabilization at a sustained plateau corresponding to 15% ± 3% of the peak translocation ($n = 19$; Fig. 7, *A* and *B*). Similar kinetics were not always observed for DAG production, and the plateau phase corresponded to 83% ± 5% of the peak amplitude ($n = 19$, Fig. 7*A*). PKCβI translocation dynamics were reminiscent of those of $[Ca^{2+}]_{pm}$, which were dominated by a pronounced initial peak caused by inositol-1,4,5-trisphosphate-mediated mobilization of Ca^{2+} from the endoplasmic reticulum, followed by a modest stable elevation, mainly reflecting store-operated Ca^{2+} entry (Fig. 7*B*) (32). The sustained PKCβI-GFP translocation probably reflects the Ca^{2+} dependence of DAG binding (33, 34). Omission of Ca^{2+} from the extracellular medium together with addition of EGTA and cyclopiazonic acid prevented the carbachol-induced rise of $[Ca^{2+}]_{pm}$ (Fig. 7*B*) and effectively prevented plasma membrane translocation of PKCβI-GFP (Fig. 7, *C* and *D*). Our findings reinforce the notion that the translocation of cPKCs is strictly

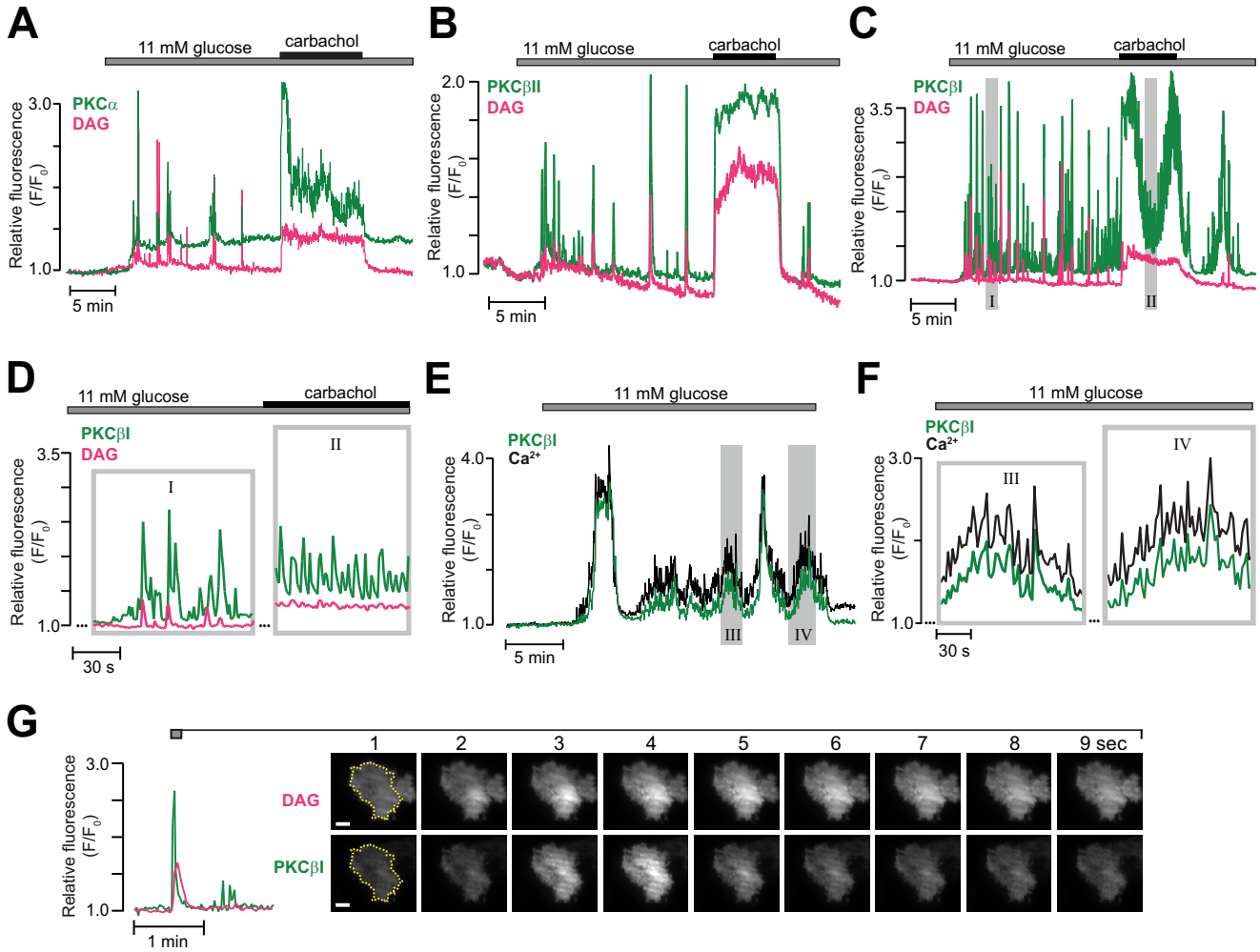

FIGURE 5. **Glucose- and carbachol-induced translocation of cPKC isoforms.** *A–C*, simultaneous TIRF recordings of DAG (*magenta*) and GFP-tagged PKC (*green*) of the α (*A*, $n = 8$ cells from three experiments), βII (*B*, $n = 6$ cells from two experiments), or βI (*C*, $n = 29$ cells from five experiments) isoforms in MIN6 cells stimulated by an increase in glucose concentration from 3 to 11 mM followed by addition of 100 μM carbachol. The regions highlighted by *shaded rectangles* are shown on an expanded time basis in *D*. *D*, time expansions of the recording from *C*. *E*, slow and fast oscillations of $[Ca^{2+}]_{pm}$ and concomitant PKCβI translocation during a step increase in glucose concentration from 3 to 11 mM (representative of seven of 14 cells in six experiments). The regions highlighted by *shaded rectangles* are shown on an expanded time basis in *F*. *F*, time expansions of the recording from *E* showing fast oscillations of PKCβI translocation and $[Ca^{2+}]_{pm}$ superimposed on slower ones. *G*, TIRF intensity recording and corresponding image pairs from the period indicated in the graph. The images were acquired every second and show that the DAG spike occurs in a restricted part of the plasma membrane and that PKCβI translocates to the same region. *Scale bars* = 5 μm.

Ca^{2+}-dependent but also emphasize that DAG mediates a fast and transient component of membrane translocation.

The Atypical Isoform PKCζ Does Not Translocate to the Plasma Membrane in Response to Muscarinic Receptor Activation, Glucose, or Insulin—We also investigated the translocation dynamics of PKCζ, an aPKC family member expressed in β cells (5–10). Although 100 μM carbachol or rise of glucose elicited pronounced DAG signaling, there was no consistent PKCζ-GFP translocation to the plasma membrane (Fig. 8*A*). A weak tendency of carbachol to increase PKCζ-GFP membrane fluorescence was probably unspecific and reproduced in control experiments with plasma membrane-anchored GFP (data not shown). Because PKCζ-GFP might be responsive to phosphatidylinositol 3,4,5-trisphosphate, we investigated the effect of insulin. At 100–300 nM, insulin induced a phosphatidylinositol 3,4,5-trisphosphate increase of similar magnitude as glucose but without recruitment of PKCζ-GFP to the plasma membrane (Fig. 8*B*).

Inhibition of $P2Y_1$ Receptors Suppresses Glucose-induced Insulin Secretion—To clarify whether DAG spiking and PKC translocation contributed to glucose-induced insulin release, we measured insulin secretion dynamics from MIN6 pseudoislets. Increase of glucose from 3 to 20 mM induced pulsatile insulin release that deteriorated after introduction of 10 μM MRS 2179 (Fig. 9*A*). After averaging data from five experiments, pulsatility was no longer evident, but there was significant suppression of insulin release during MRS 2179 exposure (time-average secretion, 64% ± 9% of the preceding 10-min control period; $p < 0.01$; Fig. 9*B*).

Discussion

This study demonstrates that exocytosis-induced microdomains of DAG recruit both conventional and nPKCs to the plasma membrane in β cells. Autocrine signaling is thus involved in controlling the spatiotemporal dynamics of PKC activity in glucose-stimulated β cells. In contrast to the view

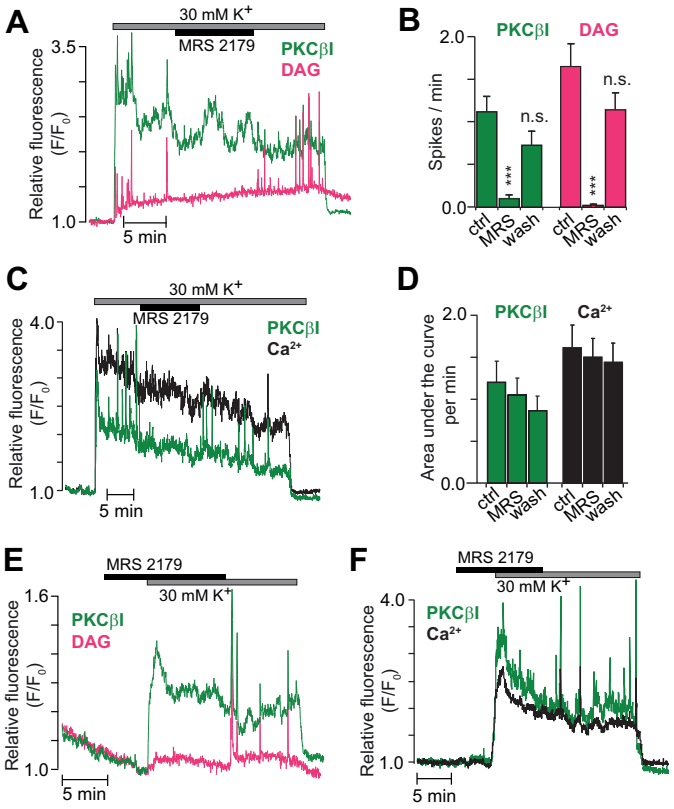

FIGURE 6. **The translocation pattern of cPKCs reflects both DAG and Ca^{2+}.** *A*, DAG dynamics (*magenta*) and PKCβI translocation (*green*) in a single MIN6 cell exposed to 3 mM glucose, 30 mM K^+, and 10 μM of the $P2Y_1$ receptor antagonist MRS 2179. *B*, means ± S.E. for the frequency of PKCβI and DAG spikes during K^+ depolarization in the presence of MRS 2179 and after washout of the drug ($n = 9$ cells from four experiments). ***, $p < 0.001$ for the difference from the high K^+ control. *ns*, not significant. *C*, PKCβI translocation (*green*) and $[Ca^{2+}]_{pm}$ (*black*) in a single cell stimulated as in *A*. *D*, means ± S.E. for the area under the curve per minute of PKCβI translocation and $[Ca^{2+}]_{pm}$ before, during, and after addition of MRS 2179 from experiments as in *C* ($n = 12$ cells from three experiments). *E* and *F*, similar experiments as in *A* and *C* but with MRS 2179 present before exposure to 30 mM K^+. $n = 10$ cells from three experiments (*E*) and 15 cells from three experiments (*F*).

that DAG changes slowly and that Ca^{2+} accounts for the rapid translocation of PKC (28, 35), this study highlights that fast, oscillatory PKC translocation can be determined by DAG spiking, whereas more sustained translocation is Ca^{2+}-dependent.

PKC translocation dynamics has previously been investigated in insulin-secreting β cells. However, glucose-induced plasma membrane recruitment of PKCβI-GFP has not been observed before, probably because of insufficient time resolution and difficulties to specifically detect changes in plasma membrane fluorescence (25). PKCα and PKCβII have been reported to undergo oscillatory membrane translocation in glucose-stimulated primary β cells (18, 23), probably reflecting slow oscillations of the free cytosolic Ca^{2+} concentration (23, 36). Endogenous PKCα has been found to strongly associate with the plasma membrane during the first phase of insulin secretion, followed by a dissociation and subsequent reassociation during second-phase insulin release (10). We now discovered more complex and rapid translocation dynamics that were strikingly parallel with DAG spiking. We propose that the previously described translocation dynamics merely reflect the Ca^{2+}-driven component of cPKC activation and that improved temporal resolution and selective imaging of the plasma membrane now reveal a superimposed component of transient, rapid, and local DAG-mediated plasma membrane binding of cPKCs. Subtle variations in translocation patterns among closely related isoforms indicate that the PKCs are fine-tuned to respond differently to distinctive DAG and Ca^{2+} signals.

Although DAG-dependent activation of nPKCs is well established, it is notable that all tested isoforms were capable to respond to glucose-induced DAG spiking with strikingly rapid translocation to the plasma membrane. Several previous studies failed to detect glucose-induced plasma membrane association of PKCδ (10, 36, 37), and in HEK293 cells, this isoform translocates to the endoplasmic reticulum after activation of purinergic receptors (38). Another study stressed a difference between the δ and ε isoforms, with PKCε translocating to the cell periphery and PKCδ to perinuclear sites in response to glucose (21). The presently observed similarity in plasma membrane translocation dynamics of the two isoforms was therefore somewhat surprising, especially because PKCδ and ε often have different or even opposing, effects (39). However, a similar spatiotemporal pattern at the plasma membrane does not exclude distinct activation at other subcellular sites. Endogenous PKCε was reported to associate with insulin staining near the nucleus, and glucose was found to induce changes in staining intensity, reflecting the biphasic insulin response of the perfused rat pancreas (10). Although the spatial resolution in the latter study did not permit a definite localization of the staining to the secretory granules, confocal imaging of PKCε-GFP supported a glucose-induced association of PKCε to insulin granules in INS1E insulinoma cells, with the most prominent effect near the plasma membrane (25). No granular pattern was evident in the presently observed PKCε distribution, indicating that the protein also can interact directly with the plasma membrane.

PKCη differed from the other nPKCs in that transient membrane translocation sometimes occurred without a simultaneously detected DAG elevation. The reason may be a higher DAG affinity of the C1 domain of PKCη compared with that of the PKCγ-derived DAG sensor (27). PKCη has been found previously to locate to the cytoplasm in rat islets (5) and to membranes in RINm5F cells (8), but, unlike in this study, carbachol did not affect the distribution pattern in either case.

The aPKCs lack a Ca^{2+}-binding C2 domain, and their C1 domain variant is unable to bind DAG (1, 2). The carbachol-induced membrane translocation is therefore likely mediated by protein-protein interactions via the PB1 domain, which is specific for aPKCs (1, 2). Carbachol-induced translocation of PKCζ to the plasma membrane has been detected previously by Western blotting and suggested to mediate carbachol-stimulated insulin release in RINm5F cells (8). Another study using various PKC inhibitors concluded that glucose-induced insulin secretion is, at least in part, dependent on activation of an aPKC isoform (20). Using immunohistochemistry, Warwar *et al.* (10) demonstrated that glucose induces transient translocation of PKCζ to the plasma membrane, corresponding to first-phase insulin secretion, and that prolonged stimulation led to accumulation of PKCζ in the nucleus. The present findings do not support the view that glucose or carbachol cause rapid association of PKCζ with the plasma membrane but do not allow

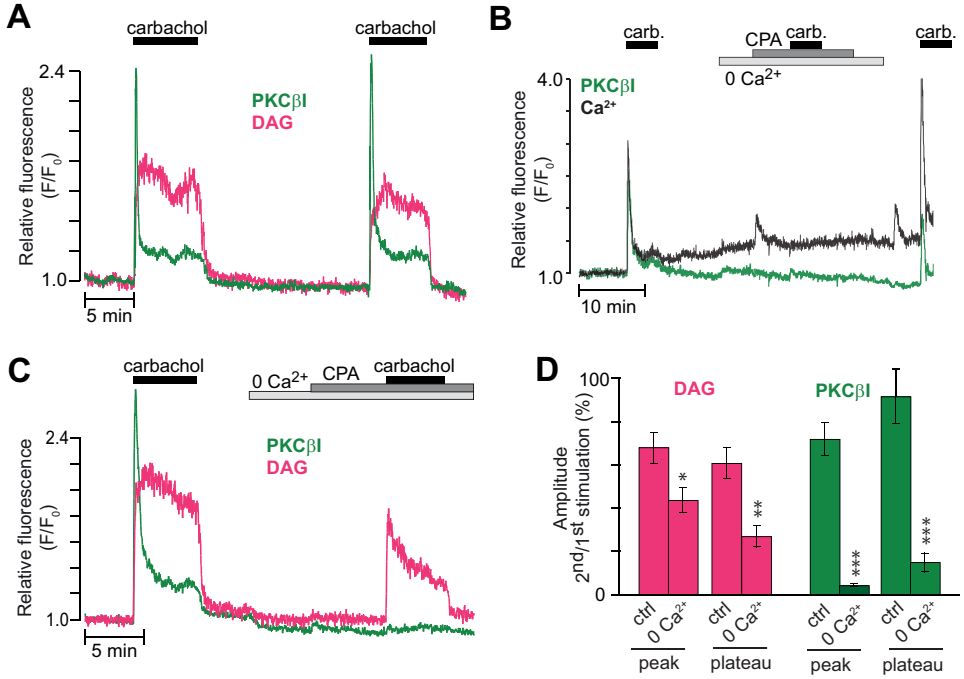

FIGURE 7. **Ca^{2+} is required for muscarinic receptor-induced translocation of cPKCs.** *A*, DAG dynamics (*magenta*) and PKCβI translocation (*green*) in response to repeated stimulations with 100 μM carbachol in the presence of 3 mM glucose. *B*, parallel recordings of $[Ca^{2+}]_{pm}$ (*black*) and PKCβI translocation (*green*) during exposure to carbachol (*carb.*) under control and Ca^{2+}-deficient conditions ($n = 22$ cells from five experiments). *CPA*, cyclopiazonic acid. *C*, similar as in *A*, but extracellular Ca^{2+} was omitted, and 2 mM EGTA and 50 μM cyclopiazonic acid were added before the second carbachol stimulation. *D*, means ± S.E. for the relative amplitudes of the peak and following plateau of simultaneously recorded DAG production and PKCβI translocation in response to two consecutive carbachol applications in the presence or absence of Ca^{2+} ($n = 18$ and 10 cells from three and two experiments for control and 0 Ca^{2+}, respectively). *, $p < 0.05$; **, $p < 0.0007$; ***, $p < 3 \times 10^{-5}$ for the difference from the control (*ctrl*).

conclusions about its localization or activity in other subcellular compartments.

Our findings strengthen the idea that DAG spiking underlies the secretagogue-induced, repetitive, brief plasma membrane associations of novel and cPKCs. They also emphasize the requirement of DAG production for nPKC translocation and suggest that cPKCs can associate with the plasma membrane without prominent increases in DAG concentration. The modest, stable DAG elevation caused by membrane depolarization in the presence of MRS 2179 (Figs. 3*B* and 6*D*) probably results from Ca^{2+}-driven phospholipase C activity (29, 40–42). Membrane binding of cPKCs is also mediated via interaction of the Ca^{2+}-binding C2 domain with other lipids, primarily phosphatidylserine, phosphatidylinositol-4,5-bisphosphate, and phosphatidylinositol 3,4,5-trisphosphate (43, 44). The C2 domain of nPKCs is not required for membrane binding. Instead, their C1 domain has an increased affinity for DAG (33). Moreover, the C1 domain binds selectively and stereospecifically to phosphatidylserine-containing membranes in a DAG-dependent manner (33, 34), which is consistent with our finding that PKCε did not translocate when DAG spiking was prevented.

The very short periods of PKC activation may explain why it has been difficult to detect increased PKC-mediated phosphorylation in glucose-stimulated β cells (18). Our data clearly show that a brief DAG spike with concomitant PKC translocation is sufficient for inducing protein phosphorylation. In β cells, the MARCKS protein seems to be phosphorylated primarily by an nPKC. The transient nature of these PKC signaling events should be suitable for regulation of rapid processes such as exocytosis. Indeed, several components of the exocytosis machinery, including SNAP25 and Munc18, are targets for PKC (45, 46). Studies of the effects of PKC inhibitors on insulin secretion have nevertheless yielded contradictory results (18–23). The inconsistencies may in part be explained by different effects of PKC on the initial and late phases of secretion (23). Another possibility is that PKC is important for the periodic pattern of insulin release. Accordingly, inhibition of the purinergic feedback mechanism that underlies the DAG spiking and transient PKC translocation markedly perturbed pulsatile insulin secretion (Fig. 9). Similar findings have been reported previously from the perifused rat pancreas using a conventional immunoassay (47) and from isolated mouse insulinoma cells using a single-cell optical assay (29). The disrupted pulsatility was associated with either inhibition (Ref. 29 and this study) or stimulation (47) of insulin secretion, a discrepancy that is probably due to differences in experimental preparations. The effects of adenine nucleotides on β cells are pleiotropic and involve the action of several purinergic receptors (reviewed in Refs. 48, 49). Recent work in human β cells confirmed that $P2Y_1$ receptors mediate autocrine stimulation of insulin secretion (50). Further investigations are required to define the functional importance of the various PKC isoforms in β cells. In conclusion, insulin secretagogues induce transient DAG microdomains that rapidly recruit both conventional and novel PKCs to the β cell plasma membrane. The findings implicate PKC signaling in the autocrine regulation of β cell function and emphasize a role of DAG for rapid kinetic control of PKC-dependent cellular processes.

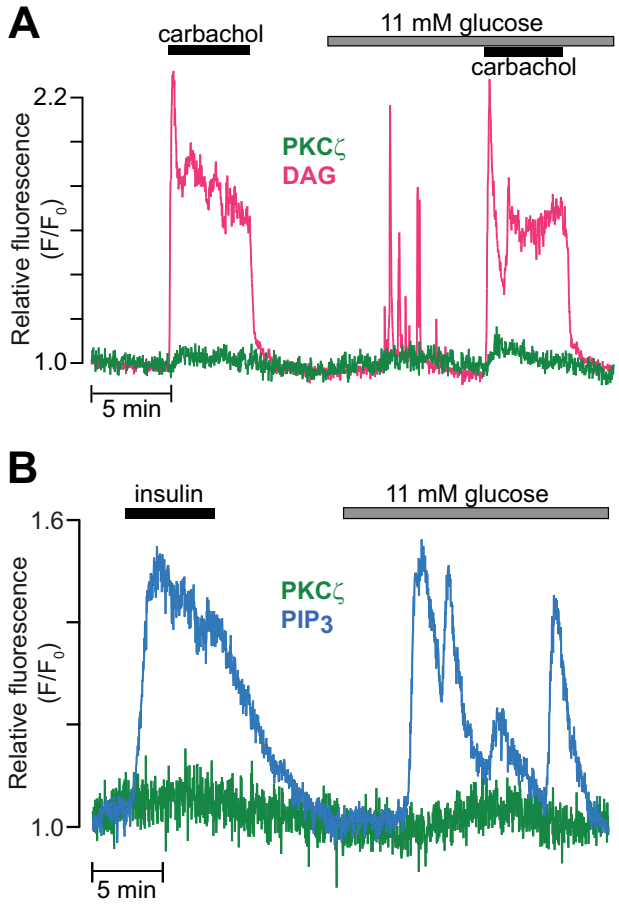

FIGURE 8. **The atypical isoform PKCζ does not translocate to the plasma membrane in response to muscarinic receptor activation, glucose, or insulin.** *A*, TIRF recording of DAG (*magenta*) and PKCζ-GFP (*green*) in a single MIN6 cell stimulated with 100 μM carbachol in the presence of 3 and 11 mM glucose ($n = 11$ cells from three experiments). *B*, TIRF recording of phosphatidylinositol 3,4,5-trisphosphate (*PIP_3*, *blue*) and PKCζ-GFP (*green*) in a MIN6 cell during exposure to 300 nM insulin and an increase in glucose concentration from 3 to 11 mM ($n = 7$ cells for 100 nM and 13 for 300 nM insulin in two experiments).

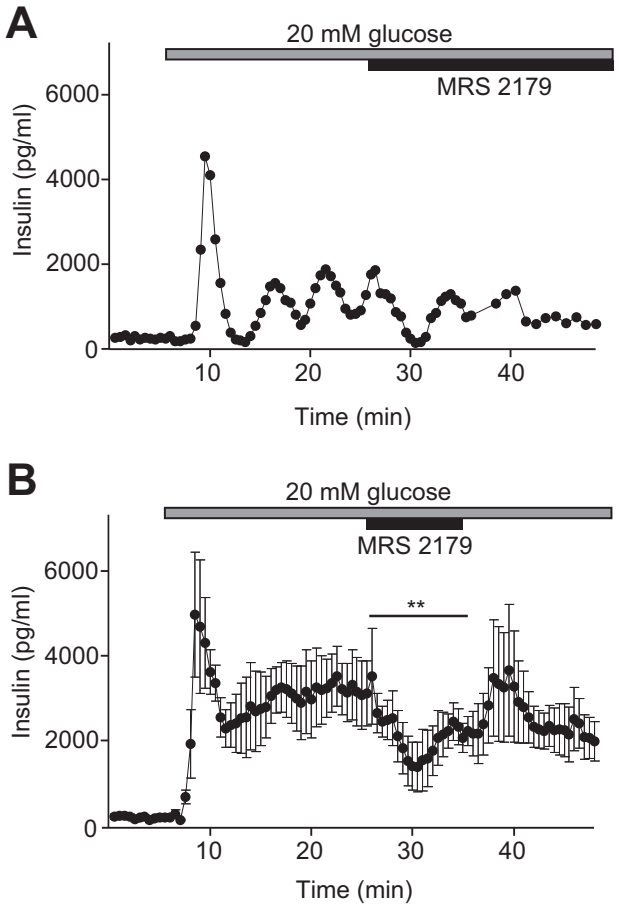

FIGURE 9. **$P2Y_1$ receptor inhibition suppresses glucose-induced pulsatile insulin secretion.** *A*, example recording of insulin secretion from a group of 20–24 superfused MIN6 pseudoislets during elevation of the glucose concentration from 3 to 20 mM and subsequent exposure to 10 μM MRS 2179. Samples were collected every 30 s for the first 38.5 min and then every 60 s. *B*, means ± S.E. from five recordings of insulin secretion in 30-s fractions from MIN6 pseudoislets exposed to 3 or 20 mM glucose and 10 μM MRS 2179. **, $p < 0.01$ refers to the difference in time-average secretion during exposure to MRS 2179 compared with that for the preceding 10-min control period.

Experimental Procedures

Reagents and DNA Constructs—MRS 2179 tetrasodium salt, MRS 2365, Gö 6976, and Gö 6983 were purchased from Tocris Bioscience (Bristol, UK). Bovine serum albumin was from Roche Diagnostics and physiological salts for the experimental buffer from Merck. Cyclopiazonic acid, EGTA, and HEPES were purchased from Sigma-Aldrich (St. Louis, MO). The plasmids containing GFP-labeled PKCs and MARCKS-GFP were provided by Prof. Tobias Meyer (Stanford University) and Prof. Naoaki Saito (Kobe University), respectively. A DAG biosensor based on the C1 domain tandem repeat in PKCγ (γC1aC1b-mCherry) was created as described earlier (29), and the genetically encoded Ca^{2+} sensor R-GECO (51) was used for measurements of the cytoplasmic Ca^{2+} concentration. mCherry targeted to the plasma membrane by a CAAX motif was used as plasma membrane marker.

Cell Culture and Transfection—If not otherwise stated, all cell culture reagents were from Life Technologies. Insulin-secreting MIN6 insulinoma cells (30) of passages 17–31 were cultured in DMEM containing 25 mM glucose and supplemented with 2 mM glutamine, 70 μM 2-mercaptoethanol, 100 units/ml penicillin, 100 μg/ml streptomycin, and 15% fetal calf serum and kept at 37 °C in a humidified atmosphere with 5% CO_2. Cells were transfected while being seeded onto 25-mm coverslips (Menzel-Gläser, Thermo Fisher Scientific, Waltham, MA) coated with polylysine (0.01 mg/ml). For each coverslip, ~0.2 million cells were suspended in 100 μl of Opti-MEM® medium containing 0.5 μl of Lipofectamine™ 2000 with up to 0.3 μg of plasmid DNA and plated onto the glass. After 3 h, when the cells were attached, the transfection was interrupted by addition of 3 ml of complete culture medium. Experiments were conducted after 13–36 h of further culture. For insulin secretion experiments, 1.5 million MIN6 cells were allowed to form pseudoislets by culture in a 60-mm polystyrol Petri dish (Sarstedt, Nümbrecht, Germany) for 4 days.

TIRF Microscopy Recordings of $[Ca^{2+}]_{pm}$, DAG, and PKC Translocation—Before each experiment, the coverslip with attached cells was transferred to experimental buffer and incubated for 30 min at 37 °C. The buffer contained 125 mM NaCl, 4.8 mM KCl, 1.3 mM $CaCl_2$, 1.2 mM $MgCl_2$, 25 mM HEPES, 3 mM D-glucose, and 0.1% (w/v) bovine serum albumin with the pH adjusted to 7.4 with NaOH. After preincubation, the coverslip

with the cells was mounted in an open 50-μl chamber and superfused with buffer at a rate of 0.3 ml/min. All experiments were performed at 37 °C.

The plasma membrane localization of GFP-tagged PKCs and the DAG translocation biosensor as well as the intensity of the Ca^{2+} sensor fluorescence were measured with a TIRF microscopy setup consisting of an Eclipse Ti microscope (Nikon) with a TIRF illuminator and a ×60, 1.45 numerical aperture objective. The 488-nm line of a multiline argon laser (ALC 60X, Creative Laser Production, Munich, Germany) and the 561-nm line from a diode-pumped solid-state laser (Jive, Cobolt AB, Solna, Sweden) were selected by narrow bandpass filters (Semrock, Rochester, NY) in a filter wheel (Sutter Instruments, Novato, CA) and used for excitation of GFP (488 nm), mCherry, and R-GECO (561 nm). Fluorescence was detected with a back-illuminated DU-897 electron multiplying charge-coupled device camera (Andor Technology, Belfast, Northern Ireland) controlled by MetaFluor software (Molecular Devices Corp., Downington, PA). Emission wavelengths were selected with a filter wheel (Sutter Instruments) and the following filters: 527/27-nm half-bandwidth for GFP and 584-nm long pass for mCherry and R-GECO (Semrock Rochester, NY). For time-lapse recordings, images or image pairs were acquired every 1 s. The laser beam was blocked by a shutter (Sutter Instruments) between image captures to minimize exposure to the potentially harmful light.

Measurements of Insulin Secretion—Groups of 20–24 pseudoislets were placed in a 20-μl chamber superfused at 130 μl/min with a similar experimental buffer as described above but with 2.6 mM $CaCl_2$. After 35 min of superfusion with buffer containing 3 mM glucose, the perifusate was collected in 30- or 60-s fractions during elevation of the glucose concentration to 20 mM and addition of MRS 2179. The collected medium was immediately put on ice, and after appropriate dilution, insulin was measured using a human insulin AlphaLISA immunodetection kit (PerkinElmer Life Sciences) according to the protocol of the manufacturer.

Data Analysis—Fluorescence intensities were logged from individual cells as a function of time using MetaFluor (Molecular Devices) and expressed relative to the initial fluorescence after subtraction of background (F/F_0). The response amplitudes and area under the curve were evaluated using Igor Pro software (Wavemetrics Inc.) and are presented as mean ± S.E. Statistical analysis was performed with paired or two-sample equal variance Student's *t* test as appropriate.

Author Contributions—A. W. and A. T. designed the study and wrote the paper. A. W. and Q. Y. performed the experiments. All authors analyzed the data and approved the final version of the manuscript.

Acknowledgments—We thank Prof. T. Meyer (Stanford University) and Prof. N. Saito (Kobe University) for expression plasmids and A. Thonig for assistance with the insulin secretion experiments.

References

1. Newton, A. C. (2010) Protein kinase C: poised to signal. *Am. J. Physiol. Endocrinol. Metab.* **298,** E395–402
2. Zeng, L., Webster, S. V., and Newton, P. M. (2012) The biology of protein kinase C. *Adv. Exp. Med. Biol.* **740,** 639–661
3. Arkhammar, P., Juntti-Berggren, L., Larsson, O., Welsh, M., Nånberg, E., Sjöholm, Å., Köhler, M., and Berggren, P. O. (1994) Protein kinase C modulates the insulin secretory process by maintaining a proper function of the β-cell voltage-activated Ca^{2+} channels. *J. Biol. Chem.* **269,** 2743–2749
4. Hashimoto, N., Kido, Y., Uchida, T., Matsuda, T., Suzuki, K., Inoue, H., Matsumoto, M., Ogawa, W., Maeda, S., Fujihara, H., Ueta, Y., Uchiyama, Y., Akimoto, K., Ohno, S., Noda, T., and Kasuga, M. (2005) PKCλ regulates glucose-induced insulin secretion through modulation of gene expression in pancreatic β-cells. *J. Clin. Invest.* **115,** 138–145
5. Ishikawa, T., Iwasaki, E., Kanatani, K., Sugino, F., Kaneko, Y., Obara, K., and Nakayama, K. (2005) Involvement of novel protein kinase C isoforms in carbachol-stimulated insulin secretion from rat pancreatic islets. *Life Sci.* **77,** 462–469
6. Kaneto, H., Suzuma, K., Sharma, A., Bonner-Weir, S., King, G. L., and Weir, G. C. (2002) Involvement of protein kinase Cβ 2 in c-myc induction by high glucose in pancreatic β-cells. *J. Biol. Chem.* **277,** 3680–3685
7. Knutson, K. L., and Hoenig, M. (1994) Identification and subcellular characterization of protein kinase-C isoforms in insulinoma β-cells and whole islets. *Endocrinology* **135,** 881–886
8. Tang, S. H., and Sharp, G. W. (1998) Atypical protein kinase C isozyme ζ mediates carbachol-stimulated insulin secretion in RINm5F cells. *Diabetes* **47,** 905–912
9. Tian, Y. M., Urquidi, V., and Ashcroft, S. J. (1996) Protein kinase C in β-cells: expression of multiple isoforms and involvement in cholinergic stimulation of insulin secretion. *Mol. Cell. Endocrinol.* **119,** 185–193
10. Warwar, N., Efendic, S., Ostenson, C. G., Haber, E. P., Cerasi, E., and Nesher, R. (2006) Dynamics of glucose-induced localization of PKC isoenzymes in pancreatic β-cells: diabetes-related changes in the GK rat. *Diabetes* **55,** 590–599
11. Biden, T. J., Schmitz-Peiffer, C., Burchfield, J. G., Gurisik, E., Cantley, J., Mitchell, C. J., and Carpenter, L. (2008) The diverse roles of protein kinase C in pancreatic β-cell function. *Biochem. Soc. Trans.* **36,** 916–919
12. Malaisse, W. J., Sener, A., Herchuelz, A., Carpinelli, A. R., Poloczek, P., Winand, J., and Castagna, M. (1980) Insulinotropic effect of the tumor promoter 12-*O*-tetradecanoylphorbol-13-acetate in rat pancreatic islets. *Cancer Res.* **40,** 3827–3831
13. Virji, M. A., Steffes, M. W., and Estensen, R. D. (1978) Phorbol myristate acetate: effect of a tumor promoter on insulin release from isolated rat islets of Langerhans. *Endocrinology* **102,** 706–711
14. Jones, P. M., Stutchfield, J., and Howell, S. L. (1985) Effects of Ca^{2+} and a phorbol ester on insulin secretion from islets of Langerhans permeabilised by high-voltage discharge. *FEBS Lett.* **191,** 102–106
15. Tamagawa, T., Niki, H., and Niki, A. (1985) Insulin release independent of a rise in cytosolic free Ca^{2+} by forskolin and phorbol ester. *FEBS Lett.* **183,** 430–432
16. Arkhammar, P., Nilsson, T., Welsh, M., Welsh, N., and Berggren, P. O. (1989) Effects of protein kinase C activation on the regulation of the stimulus-secretion coupling in pancreatic β-cells. *Biochem. J.* **264,** 207–215
17. Hii, C. S., Jones, P. M., Persaud, S. J., and Howell, S. L. (1987) A re-assessment of the role of protein kinase C in glucose-stimulated insulin secretion. *Biochem. J.* **246,** 489–493
18. Carpenter, L., Mitchell, C. J., Xu, Z. Z., Poronnik, P., Both, G. W., and Biden, T. J. (2004) PKC α is activated but not required during glucose-induced insulin secretion from rat pancreatic islets. *Diabetes* **53,** 53–60
19. Easom, R. A., Hughes, J. H., Landt, M., Wolf, B. A., Turk, J., and McDaniel, M. L. (1989) Comparison of effects of phorbol esters and glucose on protein kinase C activation and insulin secretion in pancreatic islets. *Biochem. J.* **264,** 27–33
20. Harris, T. E., Persaud, S. J., and Jones, P. M. (1996) Atypical isoforms of PKC and insulin secretion from pancreatic β-cells: evidence using Gö 6976 and Ro 31–8220 as PKC inhibitors. *Biochem. Biophys. Res. Commun.* **227,** 672–676
21. Yedovitzky, M., Mochly-Rosen, D., Johnson, J. A., Gray, M. O., Ron, D., Abramovitch, E., Cerasi, E., and Nesher, R. (1997) Translocation inhibi-

tors define specificity of protein kinase C isoenzymes in pancreatic β-cells. *J. Biol. Chem.* **272,** 1417–1420
22. Zawalich, W. S., and Zawalich, K. C. (2001) Effects of protein kinase C inhibitors on insulin secretory responses from rodent pancreatic islets. *Mol. Cell. Endocrinol.* **177,** 95–105
23. Zhang, H., Nagasawa, M., Yamada, S., Mogami, H., Suzuki, Y., and Kojima, I. (2004) Bimodal role of conventional protein kinase C in insulin secretion from rat pancreatic β-cells. *J. Physiol.* **561,** 133–147
24. Uchida, T., Iwashita, N., Ohara-Imaizumi, M., Ogihara, T., Nagai, S., Choi, J. B., Tamura, Y., Tada, N., Kawamori, R., Nakayama, K. I., Nagamatsu, S., and Watada, H. (2007) Protein kinase Cδ plays a non-redundant role in insulin secretion in pancreatic β-cells. *J. Biol. Chem.* **282,** 2707–2716
25. Mendez, C. F., Leibiger, I. B., Leibiger, B., Høy, M., Gromada, J., Berggren, P. O., and Bertorello, A. M. (2003) Rapid association of protein kinase C-ϵ with insulin granules is essential for insulin exocytosis. *J. Biol. Chem.* **278,** 44753–44757
26. Schmitz-Peiffer, C., Laybutt, D. R., Burchfield, J. G., Gurisik, E., Narasimhan, S., Mitchell, C. J., Pedersen, D. J., Braun, U., Cooney, G. J., Leitges, M., and Biden, T. J. (2007) Inhibition of PKCϵ improves glucose-stimulated insulin secretion and reduces insulin clearance. *Cell Metab.* **6,** 320–328
27. Corbalán-García, S., and Gómez-Fernández, J. C. (2006) Protein kinase C regulatory domains: the art of decoding many different signals in membranes. *Biochim. Biophys. Acta* **1761,** 633–654
28. Oancea, E., and Meyer, T. (1998) Protein kinase C as a molecular machine for decoding calcium and diacylglycerol signals. *Cell* **95,** 307–318
29. Wuttke, A., Idevall-Hagren, O., and Tengholm, A. (2013) $P2Y_1$ receptor-dependent diacylglycerol signaling microdomains in β cells promote insulin secretion. *FASEB J.* **27,** 1610–1620
30. Miyazaki, J., Araki, K., Yamato, E., Ikegami, H., Asano, T., Shibasaki, Y., Oka, Y., and Yamamura, K. (1990) Establishment of a pancreatic β-cell line that retains glucose-inducible insulin secretion: special reference to expression of glucose transporter isoforms. *Endocrinology* **127,** 126–132
31. Thore, S., Dyachok, O., Gylfe, E., and Tengholm, A. (2005) Feedback activation of phospholipase C via intracellular mobilization and store-operated influx of Ca^{2+} in insulin-secreting β-cells. *J. Cell Sci.* **118,** 4463–4471
32. Liu, Y. J., and Gylfe, E. (1997) Store-operated Ca^{2+} entry in insulin-releasing pancreatic β-cells. *Cell Calcium* **22,** 277–286
33. Giorgione, J. R., Lin, J. H., McCammon, J. A., and Newton, A. C. (2006) Increased membrane affinity of the C1 domain of protein kinase Cδ compensates for the lack of involvement of its C2 domain in membrane recruitment. *J. Biol. Chem.* **281,** 1660–1669
34. Johnson, J. E., Giorgione, J., and Newton, A. C. (2000) The C1 and C2 domains of protein kinase C are independent membrane targeting modules, with specificity for phosphatidylserine conferred by the C1 domain. *Biochemistry* **39,** 11360–11369
35. Tewson, P., Westenberg, M., Zhao, Y., Campbell, R. E., Quinn, A. M., and Hughes, T. E. (2012) Simultaneous detection of Ca^{2+} and diacylglycerol signaling in living cells. *PLoS ONE* **7,** e42791
36. Pinton, P., Tsuboi, T., Ainscow, E. K., Pozzan, T., Rizzuto, R., and Rutter, G. A. (2002) Dynamics of glucose-induced membrane recruitment of protein kinase C bII in living pancreatic islet β-cells. *J. Biol. Chem.* **277,** 37702–37710
37. Knutson, K. L., and Hoenig, M. (1996) Regulation of distinct pools of protein kinase Cδ in β-cells. *J. Cell Biochem.* **60,** 130–138
38. Hui, X., Reither, G., Kaestner, L., and Lipp, P. (2014) Targeted activation of conventional and novel protein kinases C through differential translocation patterns. *Mol. Cell. Biol.* **34,** 2370–2381
39. Duquesnes, N., Lezoualc'h, F., and Crozatier, B. (2011) PKC-δ and PKC-ϵ: foes of the same family or strangers? *J. Mol. Cell Cardiol.* **51,** 665–673
40. Biden, T. J., Peter-Riesch, B., Schlegel, W., and Wollheim, C. B. (1987) Ca^{2+}-mediated generation of inositol 1,4,5-triphosphate and inositol 1,3,4,5-tetrakisphosphate in pancreatic islets: studies with K^+, glucose, and carbamylcholine. *J. Biol. Chem.* **262,** 3567–3571
41. Tamarina, N. A., Kuznetsov, A., Rhodes, C. J., Bindokas, V. P., and Philipson, L. H. (2005) Inositol (1,4,5)-trisphosphate dynamics and intracellular calcium oscillations in pancreatic β-cells. *Diabetes* **54,** 3073–3081
42. Thore, S., Dyachok, O., and Tengholm, A. (2004) Oscillations of phospholipase C activity triggered by depolarization and Ca^{2+} influx in insulin-secreting cells. *J. Biol. Chem.* **279,** 19396–19400
43. Marín-Vicente, C., Nicolás, F. E., Gómez-Fernández, J. C., and Corbalán-García, S. (2008) The PtdIns(4,5)P_2 ligand itself influences the localization of PKCα in the plasma membrane of intact living cells. *J. Mol. Biol.* **377,** 1038–1052
44. Manna, D., Bhardwaj, N., Vora, M. S., Stahelin, R. V., Lu, H., and Cho, W. (2008) Differential roles of phosphatidylserine, PtdIns(4,5)P_2, and PtdIns(3,4,5)P_3 in plasma membrane targeting of C2 domains: molecular dynamics simulation, membrane binding, and cell translocation studies of the PKCα C2 domain. *J. Biol. Chem.* **283,** 26047–26058
45. Fisher, R. J., Pevsner, J., and Burgoyne, R. D. (2001) Control of fusion pore dynamics during exocytosis by Munc18. *Science* **291,** 875–878
46. Morgan, A., Burgoyne, R. D., Barclay, J. W., Craig, T. J., Prescott, G. R., Ciufo, L. F., Evans, G. J., and Graham, M. E. (2005) Regulation of exocytosis by protein kinase C. *Biochem. Soc. Trans.* **33,** 1341–1344
47. Salehi, A., Qader, S. S., Quader, S. S., Grapengiesser, E., and Hellman, B. (2005) Inhibition of purinoceptors amplifies glucose-stimulated insulin release with removal of its pulsatility. *Diabetes* **54,** 2126–2131
48. Petit, P., Lajoix, A. D., and Gross, R. (2009) P2 purinergic signalling in the pancreatic β-cell: control of insulin secretion and pharmacology. *Eur. J. Pharm. Sci.* **37,** 67–75
49. Tengholm, A. (2014) Purinergic $P2Y_1$ receptors take centre stage in autocrine stimulation of human β cells. *Diabetologia* **57,** 2436–2439
50. Khan, S., Yan-Do, R., Duong, E., Wu, X., Bautista, A., Cheley, S., MacDonald, P. E., and Braun, M. (2014) Autocrine activation of $P2Y_1$ receptors couples Ca^{2+} influx to Ca^{2+} release in human pancreatic β cells. *Diabetologia* **57,** 2535–2545
51. Zhao, Y., Araki, S., Wu, J., Teramoto, T., Chang, Y. F., Nakano, M., Abdelfattah, A. S., Fujiwara, M., Ishihara, T., Nagai, T., and Campbell, R. E. (2011) An expanded palette of genetically encoded Ca^{2+} indicators. *Science* **333,** 1888–1891